Table 1 Calibration coefficients and error measurements for the two PSP formulations

	PSP-A				PSP-B			
	1st	2nd	3rd	DS[a]	1st	2nd	3rd	DS[a]
Coefficient								
A	0.21	0.15	0.13	0.13	0.73	0.67	0.62	0.42
B	1.04	1.66	1.93	0.16	0.35	0.79	1.38	0.16
C	——	−0.97	−2.01	1.13	——	−0.59	−2.51	0.43
D	——	——	1.06	1.71	——	——	1.73	24.2
rmse[b]								
(inclusive)	0.0332	0.0058	0.0011	0.0004	0.0256	0.0131	0.0059	0.0002
(exclusive)	0.1038	0.0323	0.0110	0.0010	0.0447	0.0754	0.1225	0.0013

[a]DS = dual sorption. [b]rmse = root mean square error.

the initial seed values led to differences in the resulting calibration coefficients. To ensure a well-balanced calibration over a large pressure range (>1 atm), an equal number of measurements in the linear and nonlinear regions of the curve is suggested. The pressure value separating these two regions can be determined using Eq. (11):

$$B\frac{(1+DP_{\text{ratio}})^2}{CD}=1 \tag{11}$$

where $P_{\text{ratio}} = P/P_{\text{ref}}$. Using the calibration coefficients listed in Table 1, pressure ratios of 1.45 and 0.29 are calculated for PSP-A and PSP-B, respectively. Thus, additional measurements at higher pressure ratios for PSP-A and lower pressure ratios for PSP-B would further decrease the uncertainty in the corresponding calibration coefficients of those regions.

Conclusions

The application of dual sorption theory to the calibration of PSPs is presented. The nonlinear model better represents the steady-state sorption and quenching processes within the PSP coatings and yields a superior intensity–pressure calibration when applied over broad pressure ranges, in extrapolated regions, or to coatings with high luminophor loading. The tradeoff is the model's inherent nonlinearity, which requires an iterating technique for determining the calibration coefficients and leads to complications when decoupling the temperature sensitivity.[9] For high pressures and limited ranges, a second-order polynomial or linear model will suffice.

References

[1]Vieth, W. R., Howell, J. M., and Hsieh, J. H., "Dual Sorption Theory," *Journal of Membrane Science*, Vol. 1, 1976, pp. 177–220.

[2]Rogers, C. E., "Permeation of Gases and Vapours in Polymers," *Polymer Permeability*, edited by J. Comyn, Elsevier, Amsterdam, 1985, pp. 11–73.

[3]Lui, T., Campbell, B. T., Burns, S. P., and Sullivan, J. P., "Temperature- and Pressure-Sensitive Luminescent Paints in Aerodynamics," *Applied Mechanics Review*, Vol. 50, No. 4, 1997, pp. 227–246.

[4]McLachlan, B. G., and Bell, J. H., "Pressure-Sensitive Paint in Aerodynamic Testing," *Experimental Thermal and Fluid Sciences*, Vol. 10, No. 4, 1995, pp. 470–485.

[5]Morris, M. J., Donovan, J. F., Kegelmman, J. T., Schwab, S. D., Levy, R. L., and Crites, R. C., "Aerodynamic Applications of Pressure Sensitive Paint," *AIAA Journal*, Vol. 31, No. 3, 1993, pp. 419–425.

[6]Vollan, A., and Alati, L., "A New Optical Pressure Measurement System (OPMS)," *Proceedings of the 14th International Congress on Instrumentation in Aerospace Simulation Facilities*, Inst. of Electrical and Electronics Engineers, New York, 1991, pp. 10–16.

[7]James, D. R., Lui, Y.-S., Demayo, P., and Ware, W. R., "Distributions of Fluorescence Lifetimes: Consequences for the Photophysics of Molecules Absorbed on Surfaces," *Chemical Physics Letters*, Vol. 20, No. 4/5, 1985, pp. 460–465.

[8]Schanze, K. S., Carroll, B. F., Korotkevitch, S., and Morris, M., "Concerning the Temperature Dependence of Pressure Sensitive Paint," *AIAA Journal*, Vol. 35, No. 2, 1997, pp. 306–310.

[9]Hubner, J. P., Carroll, B. F., and Schanze, K. S., "Temperature Compensation Model for Pressure-Sensitive Paint," *Proceedings of the 1997 ASME Fluids Engineering Division Summer Meeting* (CD-ROM), American Society of Mechanical Engineers, New York, 1997, pp. 1–6 (Paper 3470).

G. Laufer
Associate Editor

Nonaxisymmetric Exact Piezothermoelastic Solution for Laminated Cylindrical Shell

Santosh Kapuria*
Engineers India Ltd., New Delhi 110066, India
P. C. Dumir†
Indian Institute of Technology, New Delhi 110066, India
and
S. Sengupta‡
Engineers India Ltd., New Delhi 110066, India

I. Introduction

THE electroelastic coupling in piezoelectric materials is used for active control of smart structures. Two-dimensional solutions have been presented for the thermoelectroelastic response of hybrid plates and shells, using classical and first-order shear deformation theories.[1–3] Few three-dimensional piezothermoelastic solutions are available for hybrid finite plates and shells.[4–6] These are needed to assess two-dimensional theories. Xu and Noor[6] presented three-dimensional solution for a simply supported finite cylindrical hybrid shell but did not include the case of potential difference applied across a piezoelectric layer. We present a three-dimensional solution for such a case. The governing differential equations with variable coefficients are solved by the modified Frobenius method. The constants in the general solution and the extraneous charge densities at the interfaces where potential or potential difference is prescribed are determined from the boundary and interface conditions. Results are presented to illustrate the effect of the length parameter.

II. General Solution of Governing Equations

Consider a finite circular cylindrical hybrid shell of mean radius R, thickness h, and length a, having L orthotropic layers with their principal directions along the radial, circumferential, and axial direction. The inner and outer radii are R_i, $R_o = R \mp h/2$. The innermost layer is named as the first layer. The interface between the kth and the $(k+1)$th layer is named as the kth interface. Let the thickness of the kth layer be $t^{(k)}$ and its inner radius be $R_1^{(k)}$. The layer superscript is omitted unless needed for clarity. The ends of the shell are electrically grounded, maintained at stress-free temperature, and simply supported to allow only the displacement normal to the boundary. Let u, v, w be the displacements; σ_r, σ_θ, σ_z, $\tau_{\theta z}$, τ_{zr}, $\tau_{r\theta}$ the stresses;

Received Feb. 6, 1996; revision received Nov. 10, 1996; accepted for publication July 24, 1997.

*Senior Engineer, Engineering and Technology Development (Analysis), Bhikaijee Kama Place.

†Professor, Applied Mechanics Department.

‡Chief Consultant, Engineering and Technology Development (Analysis), Bhikaijee Kama Place.

D_r, D_θ, D_z the electric displacements; ϕ the potential; and T the temperature rise from the stress-free reference temperature. We use dimensionless coordinates ξ_1, ξ_2, and $\zeta^{(k)}$ for the kth layer:

$$\xi_1 = \frac{\theta}{\pi}, \qquad \xi_2 = \frac{z}{a}, \qquad \zeta^{(k)} = \frac{r - R_1^{(k)}}{t^{(k)}}$$
$$R_1^{(k)} = R - \frac{h}{2} + \sum_{i=1}^{k-1} t^{(i)} \tag{1}$$

Let the prescribed pressure, temperature, and ϕ or D_r at the inner ($j=1$) and outer ($j=2$) surfaces be P_j, T_j, and ϕ_j or D_j. Let the number of applied potential differences be L_p with the ith one being V_i applied between the interfaces l_i and m_i with $l_i < m_i$. Let the number of interfaces with prescribed potentials be L_a with the qth one being Φ_q for the interface n_q. Thus denoting differentiation by a subscript comma, at $\xi_2 = 0$, 1,

$$u = v = 0, \qquad \sigma_z = 0, \qquad \phi = 0, \qquad T = 0 \tag{2}$$

at $r = R_i$ ($j=1$), $r = R_o$ ($j=2$),

$$\sigma_r = -P_j(\xi_1, \xi_2), \qquad \tau_{zr} = 0, \qquad \tau_{r\theta} = 0$$
$$\phi = \phi_j(\xi_1, \xi_2) \qquad \text{or} \qquad D_r = D_j(\xi_1, \xi_2) \tag{3a}$$

at $r = R_i$,

$$T = T_1(\xi_1, \xi_2) \tag{4}$$

and at $r = R_o$,

$$T = T_2(\xi_1, \xi_2)$$

$$[\phi|_{\zeta=1}]^{(m_i)} - [\phi|_{\zeta=0}]^{(l_i+1)} = V_i(\xi_1, \xi_2), \qquad i = 1, \ldots, L_p \tag{5}$$

$$[\Phi|_{\zeta=1}]^{(n_q)} = \Phi_q(\xi_1, \xi_2), \qquad q = 1, \ldots, L_a$$

The equilibrium and compatibility conditions at the interface between adjacent layers are

$$[T|_{\zeta=1}]^{(k)} = [T|_{\zeta=0}]^{(k+1)}$$
$$[k_r T_{,\zeta}|_{\zeta=1}/t]^{(k)} = [k_r T_{,\zeta}|_{\zeta=0}/t]^{(k+1)}, \qquad k = 1, \ldots, L-1 \tag{6}$$

$$[(u, v, w, \sigma_r, \tau_{r\theta}, \tau_{zr}, \phi, D_r)|_{\zeta=1}]^{(k)}$$
$$= [(u, v, w, \sigma_r, \tau_{r\theta}, \tau_{zr}, \phi, D_r)|_{\zeta=0}]^{(k+1)}$$
$$k = 1, \ldots, L-1 \tag{7a}$$

where the various k_i are the coefficients of thermal conductivity. The applied potential difference V_i induces an extraneous surface charge density, e.g., σ_i, at the interface m_i and $-\sigma_i$ at the interface l_i. The potential Φ_q applied to the interface n_q induces an extraneous surface charge density, e.g., τ_q, at this interface. The conditions (7a) for continuity of D_r need to be modified as follows. For $i = 1, \ldots, L_p$: if $m_i \neq L$, then

$$D_r^{(m_i)}\Big|_{\zeta=1} = D_r^{(m_i+1)}\Big|_{\zeta=0} - \sigma_i(\xi_1, \xi_2) \tag{7b}$$

if $l_i \neq 0$, then

$$D_r^{(l_i)}\Big|_{\zeta=1} = D_r^{(l_i+1)}\Big|_{\zeta=0} + \sigma_i(\xi_1, \xi_2) \tag{7c}$$

if $m_i = L$ and D_2 is prescribed, then Eq. (3a) for D_r is modified as

$$D_r = D_2 + \sigma_i \tag{3b}$$

if $l_i = 0$ and D_1 is prescribed, then Eq. (3a) for D_r is modified as

$$D_r = D_1 - \sigma_i \tag{3c}$$

$$[D_r|_{\zeta=1}]^{(n_q)} = [D_r|_{\zeta=0}]^{(n_q+1)} - \tau_q(\xi_1, \xi_2), \qquad q = 1, \ldots, L_a \tag{7d}$$

For the kth layer, the solution for load skew symmetric about $\theta = 0$, satisfying Eqs. (2), is taken as

$$(u, \sigma_r, \sigma_\theta, \sigma_z, \phi, D_r, T) = \sum_{m=1}^{\infty}\sum_{n=1}^{\infty}(u, \sigma_r, \sigma_\theta, \sigma_z, \phi, D_r, T)_{mn} \sin m\pi\xi_1 \sin n\pi\xi_2$$

$$(v, \tau_{r\theta}, D_\theta) = \sum_{m=1}^{\infty}\sum_{n=1}^{\infty}(v, \tau_{r\theta}, D_\theta)_{mn} \cos m\pi\xi_1 \sin n\pi\xi_2$$

$$\tau_{\theta z} = \sum_{m=1}^{\infty}\sum_{n=1}^{\infty}\tau_{\theta z mn} \cos m\pi\xi_1 \cos n\pi\xi_2 \tag{8}$$

$$(w, \tau_{zr}, D_z) = \sum_{m=1}^{\infty}\sum_{n=1}^{\infty}(w, \tau_{zr}, D_z)_{mn} \sin m\pi\xi_1 \cos n\pi\xi_2$$

$$(P_i, \phi_i, D_i, T_i, V_i, \Phi_i, \sigma_i, \tau_i) = \sum_{m=1}^{\infty}\sum_{n=1}^{\infty}(P_i, \phi_i, D_i, T_i, V_i, \Phi_i, \sigma_i, \tau_i)_{mn} \sin m\pi\xi_1 \sin n\pi\xi_2$$

Let S_{ij}, d_i, ϵ_i, α_i, and q_1 be the elastic compliances, piezoelectric strain constants, dielectric constants, coefficients of thermal expansion, and pyroelectric constant. The nine constitutive equations[2] for orthorhombic material of class mm2, with poling in the radial direction, and four equilibrium equations of force and charge are transformed into five algebraic equations for σ_θ, σ_z, $\tau_{\theta z}$, D_θ, and D_z and the following eight differential equations for u, v, w, σ_r, $\tau_{r\theta}$, τ_{zr}, ϕ, and D_r. With $X_{mn} = [u \;\; v \;\; w \;\; \sigma_r \;\; \tau_{r\theta} \;\; \tau_{zr} \;\; \phi \;\; D_r]^T_{mn}$,

$$X_{mn,r} = \left(A_0 + A_1/r + A_2/r^2\right)X_{mn} + (Q_0 + Q_1/r)T_{mn} \tag{9}$$

The expressions of A_0, A_1, A_2, Q_0, and Q_1 are not listed for brevity.

Using the expansion (8) for T, the heat conduction equation reduces to

$$T_{mn,rr} + T_{mn,r}/r - \mu_m^2 T_{mn}/r^2 - \mu_n^2 T_{mn}/R_1^2 = 0$$
$$\mu_m = m(k_\theta/k_r)^{\frac{1}{2}}, \qquad \mu_n = n\pi R_1(k_z/k_r)^{\frac{1}{2}}/a \tag{10}$$

The modified Frobenius method is used to solve Eqs. (10) and (9). The general solution of Eq. (10) is

$$T_{mn}(\zeta) = \sum_{j=1}^{2} e^{\rho_j \zeta}\left(\sum_{i=0}^{\infty} T_{mni}^j \zeta^i\right)A_j^{mn} \tag{11}$$

where A_j^{mn} are arbitrary constants and

$$\rho_1, \rho_2 = \left\{-1 \pm \left[1 + 4\left(\mu_m^2 + \mu_n^2\right)\right]^{\frac{1}{2}}\right\}/2s$$
$$s = R_1/t, \qquad T_{mn0}^j = 1, \qquad T_{mn1}^j = T_{mn2}^j = 0$$

The term T_{mni}^j ($i > 2$) is obtained recursively by equating the coefficient of ζ^{i-2} in Eq. (10) to zero.

The complementary solution $X_{mn}^c(\zeta)$ of Eq. (9) is taken as

$$X_{mn}^c(\zeta) = e^{\lambda\zeta}\sum_{i=0}^{\infty} Y_i \zeta^i \tag{12}$$

where

$$Y_1 = 0, \qquad AY_0 = \lambda Y_0, \quad \text{and} \qquad A = [A_0 R_1 + A_1 + A_2/R_1]/s$$

The terms λ and Y_0 form an eigenpair of matrix A, and Y_i^j for each eigenpair (λ_j, Y_0^j) is recursively obtained as before. The complementary solution for eigenvalues $\lambda_1, \lambda_2 = \alpha \pm i\beta$ with eigenvector Y_0^1 for λ_1 is expressed in terms of two real constants C_1^{mn} and C_2^{mn} as

$$X_{mn}^c(\zeta) = F_1^{mn}(\zeta)C_1^{mn} + F_2^{mn}(\zeta)C_2^{mn} \tag{13}$$

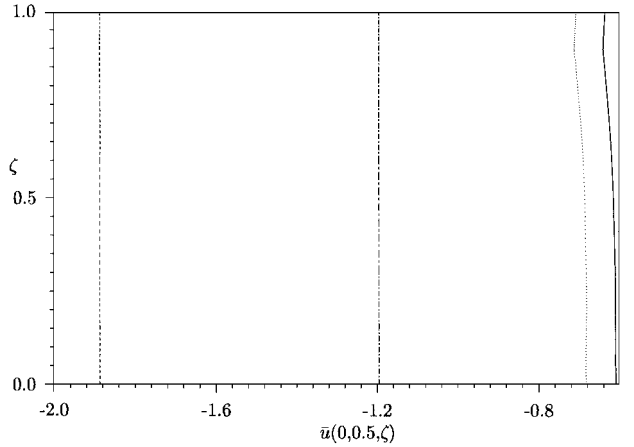

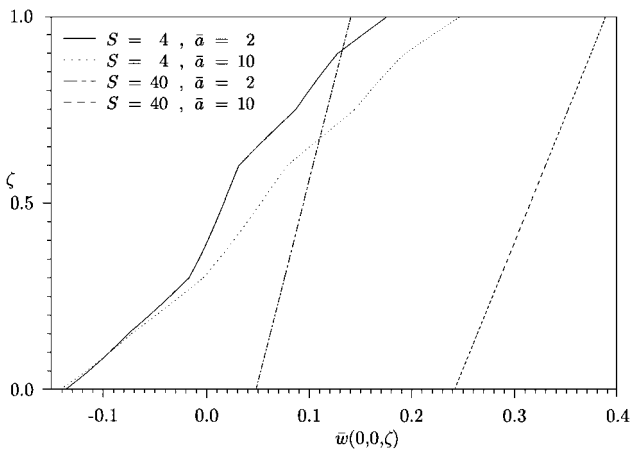

Fig. 1 Distributions of $\bar{u}$ and $\bar{w}$ for load case 1.

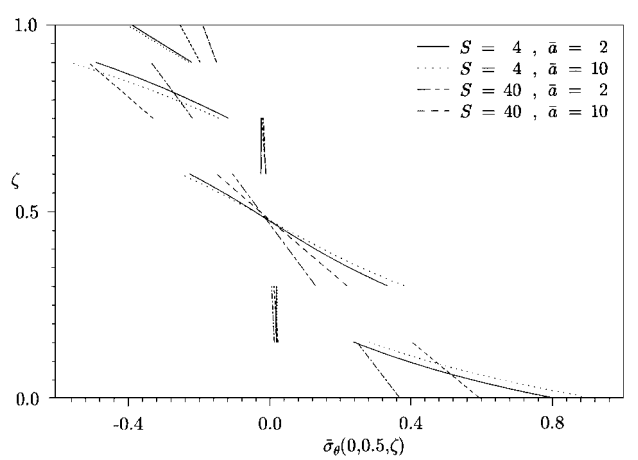

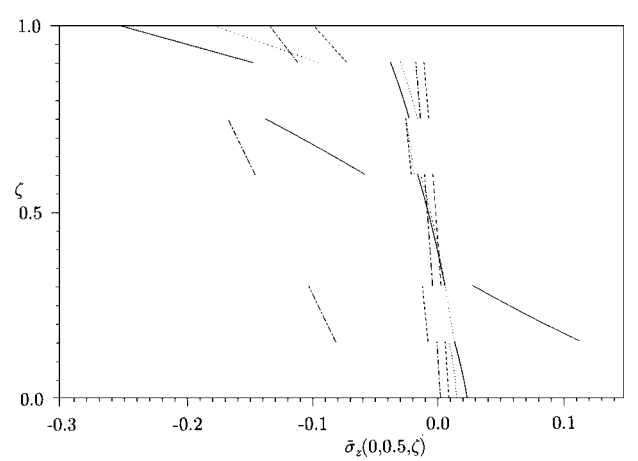

Fig. 2 Distributions of $\bar{\sigma}_\theta$ and $\bar{\sigma}_z$ for load case 1.

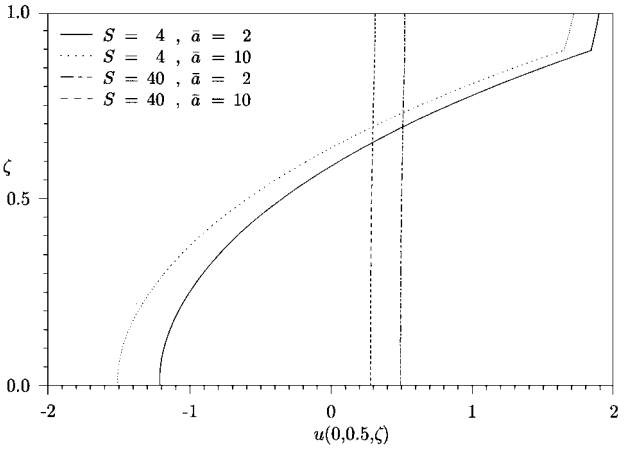

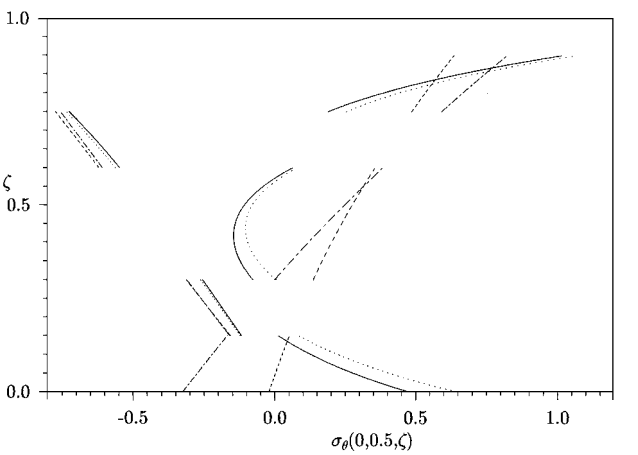

Fig. 3 Distributions of $\hat{u}$ and $\hat{\sigma}_\theta$ in the substrate for load case 2.

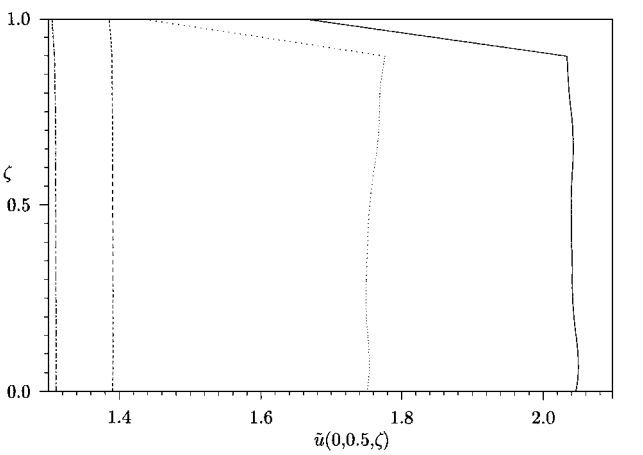

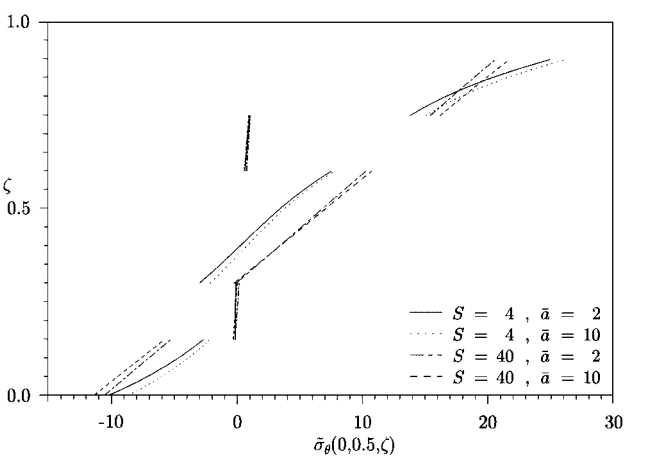

Fig. 4 Distributions of $\tilde{u}$ and $\tilde{\sigma}_\theta$ in the substrate for load case 3.

with

$$F_1^{mn} = e^{\alpha\zeta}\left[\cos\beta\zeta\sum_{i=0}^{\infty}\Re\left(Y_i^1\right)\zeta^i - \sin\beta\zeta\sum_{i=0}^{\infty}\Im\left(Y_i^1\right)\zeta^i\right]$$

$$F_2^{mn} = e^{\alpha\zeta}\left[\sin\beta\zeta\sum_{i=0}^{\infty}\Re\left(Y_i^1\right)\zeta^i + \cos\beta\zeta\sum_{i=0}^{\infty}\Im\left(Y_i^1\right)\zeta^i\right]$$

The terms $\Re$ and $\Im$ indicate the real and imaginary parts of a complex number. Thus the complete solution X_{mn} is

$$X_{mn}(\zeta) = \sum_{j=1}^{8} F_j^{mn}(\zeta)C_j^{mn} + \sum_{j=1}^{2} G_j^{mn}(\zeta)A_j^{mn}$$
$$\text{with} \quad G_j^{mn}(\zeta) = e^{\rho_j\zeta}\left(\sum_{i=0}^{\infty} Z_i^j\zeta^j\right) \tag{14}$$

where $F_j^{mn}(\zeta)$ is given by Eq. (13) and C_j^{mn} are real constants. The various Z_i^j are obtained by a recursive relation, which is omitted here for brevity. The infinite power series in $F_j^{mn}(\zeta)$ and $G_p^{mn}(\zeta)$ are truncated such that the contribution of the first neglected term is less than 10^{-10}.

The $2L$ constants $(A_j^{mn})^{(k)}$ for L layers are determined from the $2L$ thermal conditions (4) and (6). The $8L$ constants $(C_j^{mn})^{(k)}$ for L layers and $L_p + L_a$ unknown extraneous surface charge densities $\sigma_{i_{mn}}$ and $\tau_{q_{mn}}$ are obtained from $8L + L_p + L_a$ conditions (3), (5), and (7).

III. Numerical Results and Conclusions

Consider a shell made of cross-ply graphite-epoxy laminate $[0/90/0]_s$ and a layer of lead zirconate titanate (PZT)-5A of thickness $h/10$, bonded to its outer surface. The orientation of the fibers is given relative to the θ direction. All plies of the substrate have equal thickness. The material properties are selected as in Ref. 6. The interface of the piezoelectric layer with the substrate is grounded. Loads with the following nonzero P_i, T_i, or ϕ_i are considered: 1) $P_2 = p_0\cos 4\pi\xi_1\sin\pi\xi_2$, 2) $T_2 = T_0\cos 4\pi\xi_1\sin\pi\xi_2$, and 3) $\phi_2 = \phi_0\cos 4\pi\xi_1\sin\pi\xi_2$. The results for the three cases are nondimensionalizedas follows with $\bar{a} = a/R$, $S = R/h$, $d_T = 374\times 10^{-12}\,\text{CN}^{-1}$, $\alpha_T = 22.5\times 10^{-6}\,\text{K}^{-1}$, $E_T = 10.3$ GPa:

$$1)\ (\bar{u},\bar{w}) = 10(u,\bar{a}w)E_T/hS^3p_0, \quad (\bar{\sigma}_\theta,\bar{\sigma}_z) = (\sigma_\theta,\sigma_z)/S^2p_0$$
$$2)\ \hat{u} = 100u/h\alpha_T S^2T_0, \quad \hat{\sigma}_\theta = \sigma_\theta/\alpha_T E_T T_0$$
$$3)\ \tilde{u} = 10u/S^2d_T\phi_0, \quad \tilde{\sigma}_\theta = \sigma_\theta h/E_T d_T\phi_0$$

The effect of the length parameter $\bar{a}$ is studied for thick ($S = 4$) and thin ($S = 40$) shells.

The through-the-thickness distributions of some entities for the pressure load case 1 are shown in Figs. 1 and 2. It is observed from Fig. 1 that the deflection $\bar{u}$ is almost uniform for thin shells with $S = 40$. The variation of the axial displacement $\bar{w}$ across the thickness is linear for the thin shells and is piecewise linear for thick shells. The distributions of the predominant stresses $\bar{\sigma}_\theta$ and $\bar{\sigma}_z$, shown in Fig. 2, reveal that the relative increase of $\bar{\sigma}_\theta$ with $\bar{a}$ is less for the thick shell compared with the thin shell.

The results for thermal load case 2 are given in Fig. 3. The distribution of $\hat{u}$ across the whole thickness is almost uniform for thin shells with $S = 40$. For thick shells, the distribution of $\hat{u}$ and $\hat{\sigma}_\theta$ across the elastic substrate is nonlinear. The distributions of $\tilde{u}$ and $\tilde{\sigma}_\theta$ are presented in Fig. 4 for the potential load case 3. The variation of $\tilde{u}$ in the piezoelectric layer is linear. The variation of $\tilde{\sigma}_\theta$ for thick shells is relatively less nonlinear compared with thermal load case 2.

It is inferred from the results that the displacements and the predominant normal stresses in the substrate are significantly affected by the radius to thickness ratio but the nature of their through-the-thickness distributions is not affected much by the length-to-radius ratio for both thick and thin shells.

References

[1]Tauchert, T. R., "Piezothermoelastic Behavior of a Laminated Plate," *Journal of Thermal Stresses*, Vol. 15, No. 1, 1992, pp. 25–37.

[2]Jonnalagadda, K. D., Blandford, G. E., and Tauchert, T. R., "Piezothermoelastic Behavior of a Laminated Plate," *Computers and Structures*, Vol. 51, No. 1, 1994, pp. 79–89.

[3]Tzou, H. S., and Ye, R., "Piezothermoelastic and Precision Control of Piezoelectric Systems, Theory and Finite Element Analysis," *Journal of Vibration and Acoustics*, Vol. 116, No. 4, 1994, pp. 489–495.

[4]Xu, K., Noor, A. K., and Tang, Y. Y., "Three-Dimensional Solutions for Coupled Thermoelectroelastic Response of Multilayered Plates," *Computer Methods in Applied Mechanics and Engineering*, Vol. 126, No. 4, 1995, pp. 355–371.

[5]Kapuria, S., Sengupta, S., and Dumir, P. C., "Three Dimensional Solution for Simply-Supported Piezoelectric Cylindrical Shell for Axisymmetric Load," *Computer Methods in Applied Mechanics and Engineering*, Vol. 140, No. 2, 1997, pp. 139–155.

[6]Xu, K., and Noor, A. K., "Three-Dimensional Analytical Solutions for Thermoelectroelastic Response of Multilayered Cylindrical Shells," *AIAA Journal*, Vol. 34, No. 4, 1996, pp. 802–812.

R. K. Kapania
Associate Editor

Effective Mass Sensitivities for Systems with Repeated Eigenvalues

Antonio Paolozzi*
University of Rome "La Sapienza," 00185 Rome, Italy
and
Ludek Pesek†
Academy of Sciences of Czech Republic, 18200 Prague 8, Czech Republic

Introduction

THE effective modal mass, commonly referred to as effective mass, is quite important in characterizing the dynamical behavior of a base driven structure because it allows the reduction of complex structures to equivalent spring-mass systems[1,2] and the identification of the modes that can be significantly excited through the interface by the base motion. These modes are called target modes, and they have to be well correlated to the experimental ones to obtain a test verified finite element (FE) model.[3] The effective mass sensitivities, on the other hand, can be used in optimization problems such as that of finding the optimal position of an extra payload to be added[4,5] or that of the minimization of errors between experimental and numerical effective masses. In this work the calculation of effective mass sensitivities has been generalized to the case of repeated eigenvalues.

Theory

The definition of effective mass matrix is[2,6]

$$\boldsymbol{M}_{\text{eff}_i\,(r\times r)} = \left(\boldsymbol{X}_R^T\boldsymbol{M}\boldsymbol{x}_i\right)\left(\boldsymbol{x}_i^T\boldsymbol{M}\boldsymbol{X}_R\right) \tag{1}$$

where r is the number of rigid body modes of the structure, $\boldsymbol{X}_R$ is the rigid body mode matrix, $\boldsymbol{x}_i$ is the ith eigenvector of the eigenvalue problem

$$(\boldsymbol{K} - \lambda_i\boldsymbol{M})\boldsymbol{x}_i = 0 \tag{2}$$

$\boldsymbol{M}$ and $\boldsymbol{K}$ are the mass and stiffness matrices of the FE model of the structure, and λ_i is the ith eigenvalue. By differentiating Eq. (1)

Received Nov. 18, 1996; revision received June 30, 1997; accepted for publication July 3, 1997.

*Assistant Professor, Aerospace Department.
†Researcher, Institute of Thermomechanics.